ISSN: 2277-9655
Impact Factor: 5.164
CODEN: IJESS7

IJESRT
INTERNATIONAL JOURNAL OF ENGINEERING SCIENCES & RESEARCH TECHNOLOGY

# SYNTHESIS, CHARACTERIZATION AND *IN VITRO* CYTOTOXICITY EVALUATION OF PEGYLATED MN DOPED ZNO NANOPARTICLES ON HUMAN CERVICAL CANCER HELA CELLS

**G. Vijayakumar[1], G. Bhoopathi[*2]**
[1&*2]Department of Physics, PSG College of Arts and Science, Coimbatore – 641 014

**DOI**: 10.5281/zenodo.1241422

## ABSTRACT
The aim of the present study was to investigate the *in vitro* cytotoxicity of PEGylated Mn doped ZnO nanoparticles against the Human Cervical Cancer HeLa Cells. Pure and Mn (2.0, 2.5 and 3.0%) doped ZnO nanoparticles were synthesized by chemical precipitation method. The structural and morphological interpretations of the as prepared nanoparticles were carried out using X-Ray Diffraction (XRD), UV-Vis DRS Spectroscopy, Photoluminescence Spectra and Field Emission Scanning Electron Microscopy (FESEM) techniques. The cytotoxicity mechanisms of the as prepared nanoparticles were investigated against the Human Cervical Cancer HeLa Cells by observing the cell penetration ratio, cell viability and ROS generation. It was observed that, among the four nanoparticles (znsp1, znsp2, znsp3 and znsp4) 2.0% Mn doped ZnO nanoparticles exhibited higher cell killing activity. The cytotoxicity results showed that pure and Mn doped ZnO nanoparticles exert distinctive killing effects on Human Cervical Cancer HeLa Cells while posing minimal impact on normal cells.

**KEYWORDS**: ZnO nanoparticles, anticancer activity, Human Cervical Cancer HeLa Cells.

## I. INTRODUCTION
Potential application of nanomaterials in biotechnology merges the fields of material science and biology. The reason behind the intense interest is that nanotechnology enables controlled synthesis of materials where at least one dimension of the structure is < 100 nm. The size reduction of materials to the nanoscale subsequently alters their electrical, magnetic, structural and chemical properties promoting distinctive interactions with cell biomolecules, enabling physical transport into the internal structures of cells. Engineered nanostructures have gained much importance in various fields and have been applied both in biological and biomedical engineering [1]. These materials in general possess larger availability of surface atoms, which can lead to increased surface reactivity, and can maximize their ability to be loaded with therapeutic agents to deliver them to target cells. By appropriate engineering design, these nanomaterials can acquire the ability to target selectively agents for the treatment of cancer. ZnO is a conventional wide band-gap semiconductor that has been greatly explored in multiple areas of science. Although ZnO nanoparticles have been utilized by multidisciplinary research community for several years, they have only been explored recently for cancer applications [2]. Among several photosensitizers, the unique optical and electronic property of Zinc Oxide nanoparticle makes them more favorable in triggering in-vitro cell-killing effect by photocatalytic effects. Upon UV irradiation, ZnO nanoparticle absorbs maximum quantity of radiation and stimulates ROS (Reactive oxygen species) generation such as hydroxyl radical and superoxide, causing oxidative injury and cell death. ZnO nanoparticles are stable and their synthesis is inexpensive but agglomeration of chemically synthesized nanoparticles due to high surface energy results in their size increase as well as instability. Its ultimate solution is capping with polymeric modifying agents or surfactants like polyethylene glycol (PEG), polyethylene oxide (PEO) and polyvinyl pyrrolidone (PVP) [3-6]. Capping approach results in significant size reduction of nanoparticles contributing to their stability.
Our present study was formulated to investigate the anticancer activity of Polyethylene glycol - PEG encapsulated pure and Mn doped ZnO nanoparticles (Mn concentrations 2.0%, 2.5% and 3.0%) against Human Cervical Cancer HeLa Cells. The PEG functionalized pure and Mn doped ZnO nanoparticles were synthesized by chemical precipitation method and labeled as Znsp1 (Pure ZnO), Znsp2 (ZnO:Mn - 2.0%), Znsp3 (ZnO:Mn -

ISSN: 2277-9655
Impact Factor: 5.164
CODEN: IJESS7

2.5%) and Znsp4 (ZnO:Mn - 3.0%). Here, the bio-compatible capping agent PEG has been used to control the particle size and to minimize the surface defects of the as prepared nanoparticles.

## II. MATERIALS AND METHODS

### 2.1 Materials

All the reagents were of analytical grade and were used without further purification. Zinc acetate dihydrate ($Zn(CH_3COO)_2.2H_2O$), sodium hydroxide (NaOH), manganese acetate tetra hydrate ($Mn(CH_3COO)_2.4H_2O$), and Polyethylene glycol (PEG-6000) were used as received to prepare Mn doped ZnO, and PEG encapsulated Mn doped ZnO nanoparticles. Throughout the process ethanol water was used as solvent.
Biological reagents used for experiments with cells, such as RPMI 1640 medium, fetal bovine serum(FBS), Penicillin/streptomycin, 2,7-dichlorofluoroscein diacetate (DCFH-DA, 97%), 3-(4,5- dimethylthiazol-2-yl)-2,5-diphenyltetrazolium bromide (methyl tetrazolium, MTT, 97.5%) and phosphate-buffered saline (PBS, pH 7.4) were purchased from Sigma-Aldrich.

### 2.2 Preparation of Pure and Mn doped ZnO Nanoparticles

Zinc acetate dihydrate ($Zn(CH_3COO)_2.2H_2O$) (0.5M) was dissolved in 50 ml ethanol and stirred for 30minutes at room temperature. Meanwhile, PEG solution was prepared by dissolving 100 mg in 20 ml ethanol and was added to the above solution. Sodium hydroxide NaOH (1 M) was prepared separately and was added dropwise into the above solution under constant stirring. After being stirred at room temperature for 2–3 h, the as formed precipitates were filtered, washed several times with distilled water and ethanol and finally dried in hot air oven at 80ºC to get PEG modified ZnO nanoparticles. The entire reaction was carried out with pH 10.
The Mn doped ZnO nanoparticles were prepared along with a capping agent to control both the size and the shape of the prepared nanomaterials. The manganese precursor (2 wt%) ($(CH_3COO)_2Mn{\cdot}4H_2O$) was dissolved in 100 ml of ethanol and stirred for 2 hours which forms solution A. Meanwhile 0.5M Zinc acetate dihydrate [$Zn(CH_3(COO))_2 2H_2O$] was dissolved in 50 ml of ethanol and stirred for 30 minutes which forms solution B. Then solution A and B are mixed together and the temperature was raised to 50 °C and the solution was stirred again. Finally, the required amount of PEG was added as a capping agent. The mixture was then kept stirring for 3 hours and then hydrolyzed by adding NaOH under ultrasonication for 2 hours. The resulting mixture was washed with distilled water and ethanol and finally dried in hot air oven at 200ºC to get PEG functionalized Mn doped ZnO nanoparticles.

### 2.3 Cytotoxicity Analysis

#### 2.3.1 MTT Assay

The anticancer activity of the pure and Mn doped ZnO nanoparticles were determined using standard MTT assay method. The dose response of Human Cervical Cancer HeLa Cells for the pure and Mn doped nanoparticles with different Mn concentrations were analysed using the MTT assay. All the four test nanoparticles znsp1, znsp2, znsp3 and znsp4 each with concentrations 20, 40, 60, 80 and 100 µg/ml were exposed to the cells.

#### 2.3.2 Cytotoxicity studies

The cervical cancer cells were seeded into 24-well plates at a density of $1x10^5$ cells/well and were incubated for 24 hours. Pure and Mn doped ZnO nanoparticles were suspended in RPMI 1640 medium to get the final concentrations of 20, 40, 60, 80 and 100 µg/L and then all the nanoparticle stock solutions were ultrasonicated for 30 min to reduce agglomeration. Each of the five concentrations of nanoparticles znsp1, znsp2, znsp3 and znsp4 were added to the test cells. Following the exposure of 24 h, cell viability was measured by MTT assay. MTT was dissolved in PBS at 5 mg/mL, and then 20 µL of this solution was added to each well cultured at 37 °C under a humidified atmosphere with 5% $CO_2$ for 24 hours. The medium was then removed, and washed with Phosphate saline solution. After this 100 $\mu$L of DMSO was added into each well to dissolve the metabolites of MTT. The viable cells were determined by the absorbance at 570nm by microplate reader.

## III. RESULTS AND DISCUSSION

### 3.1 Structural Analysis

The XRD pattern of the PEG encapsulated pure ZnO nanoparticle is shown in Figure 1. The spectra clearly shows the diffraction peaks in pattern indexed as the ZnO with lattice constants a = 3.249 and c = 5.206 Å and well matched with the JCPDS, No. 36-1451. The peaks are observed at $2\theta$ = 31.78°, 34.48° and 36.25°, corresponding to (100), (002), (101) reflections of the wurtzite structure ZnO, respectively. No significant

ISSN: 2277-9655
Impact Factor: 5.164
CODEN: IJESS7

characteristic peaks of impurities could be detected. The broad diffraction peaks (around 2θ = 20°) indicated that the strong interaction between PEG and ZnO. Furthermore, the grain size of the ZnO nano could be calculated as 23 nm according to the Scherrer formula D = Kλ/(βcosθ), where K is the scherrer constant, λ the X-ray wavelength, β the peak width of half maximum, and θ is the Bragg diffraction angle. It was observed that the addition of capping agent plays a vital role in controlling the growth of the crystal during the synthesis of ZnO nanoparticles [7]. It has been observed that the PEG encapsulated ZnO:$Mn^{2+}$ nanoparticles were more intense and sharper implying a good crystalline nature of the as synthesized ZnO products. In addition, the broadening of the diffraction peaks also denotes that the crystallite sizes were small as a result of Mn doping and capping of PEG. These results show that PEG6000 plays an important role in controlling the ZnO particles size.

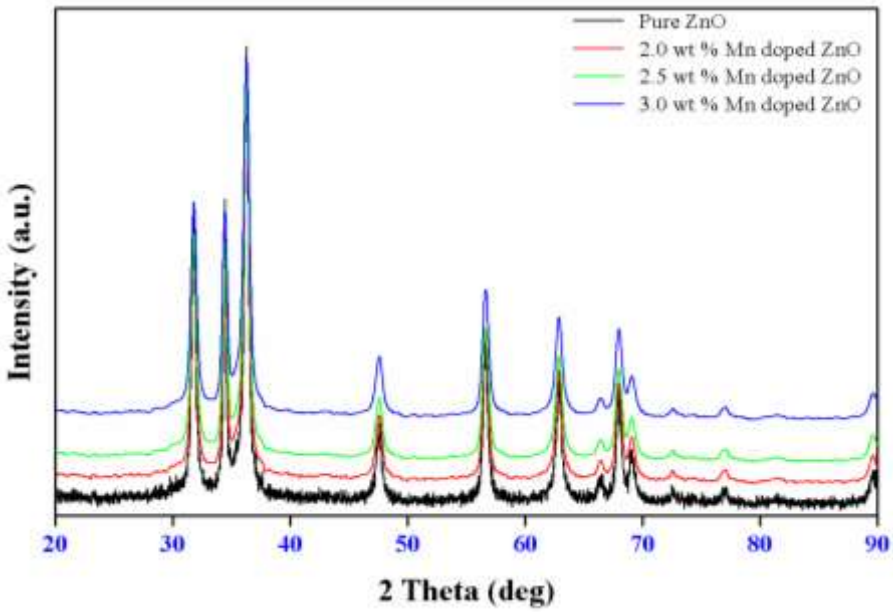


**Figure 1: XRD Pattern of Pure and Mn doped ZnO nanoparticles**

Lattice parameters has been calculated and has been shown in the Table 1 shows that the lattice constants of Mn doped ZnO were slightly larger than those of undoped ZnO, because the ionic radius of Mn(II) (0.66) is larger than that of Zn(II) (0.60). The length of both *a* and *c* axis expands with increasing Mn doping in ZnO. The expansion of the lattice constants and the slight shift of XRD peaks of different concentration of Mn doped ZnO indicated that manganese has exactly doped into the ZnO structure.

**Table 1: The lattice constants of pure and Mn doped ZnO**

| **Lattice Constants** | **ZnO** | **Mn doped ZnO** | | |
|---|---|---|---|---|
| | | **2.0% Mn** | **2.5% Mn** | **3.0% Mn** |
| a (Å) | 3.248 | 3.255 | 3.270 | 3.277 |
| b (Å) | 5.204 | 5.212 | 5.236 | 5.243 |

The average crystal size (D) was estimated using the Scherrer formula. The crystal size of the ZnO decreases on doping 2.0% of Mn and on subsequent doping shows an increasing tendency as shown in table 2.

**Table 2: Average grain size as a function of Mn in ZnO**

| **Grain size (D) nm** | | | |
|---|---|---|---|
| **Pure ZnO** | **2.0% Mn doped ZnO** | **2.5% Mn doped ZnO** | **3.0% Mn doped ZnO** |
| 19.11 | 15.45 | 17.88 | 18.24 |

ISSN: 2277-9655
Impact Factor: 5.164
CODEN: IJESS7

**3.2 UV-Vis (DRS) Analysis:**

The UV-VIS Diffuse reflectance spectra (DRS) of pure and Mn doped zinc oxide nanoparticles are shown in Figure 2. The DRS spectrum of the pure ZnO shows the absorption peak at 410 nm which can approximately estimated to have band gap energy around 3.6 eV. The band gap of bulk ZnO is around 3.3 eV. This diminution might be due to the quantum confinement, which is in good agreement with the reduced mean particle size values calculated from the X-Ray diffraction measurements. Compared to the DRS spectra of the pure ZnO nanoparticles, 2.0% Mn doped ZnO shows appreciable shift in the absorption wavelength to 2.87 eV. This shift in absorption indicates that the 2.0% Mn content modifies the crystal structure of pure ZnO. Similar trend was observed for 2.5 and 3.0% Mn doped ZnO nanoparticles [8, 9]. The shift in the absorption wavelengths of 2.82 eV and 2.64 eV were assigned to 2.5% and 3.0% Mn doped ZnO nanoparticles respectively. It was observed that the addition of capping agent plays a vital role in controlling the growth of the crystal during the synthesis of Mn doped ZnO nanoparticles. These results imply that addition of $Mn^{2+}$ into the ZnO lattice shifts the bandgap to the visible region which enhances its photocatalytic property.

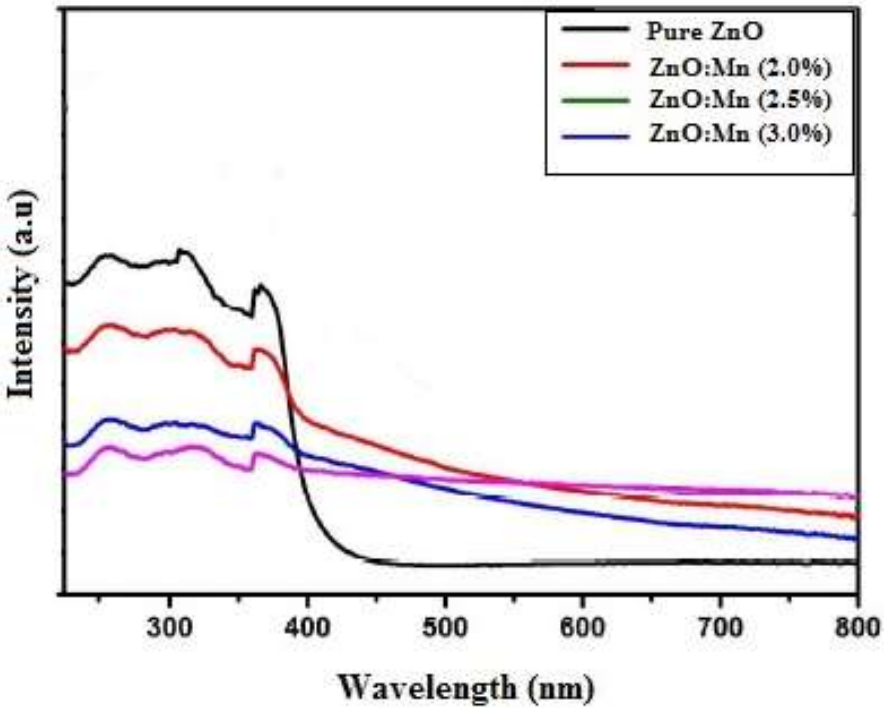


**Figure – 2 Diffused reflectance spectra of Pure and Mn doped ZnO nanoparticles**

**3.3 Photoluminescence Studies**

The optical emission properties of the ZnO:Mn2+ nanoparticles ( 2.0, 2.5 and 3.0% Mn) were investigated by PL spectroscopy. In Figure 3 two characteristic PL bands emerged: the near band edge emission in the UV region, which has originated due to the recombination of free excitons through an exciton-exciton collision process, and the other deep level emission in the visible region, caused by impurities and structural defects of the crystal [10, 11]. The pure ZnO nanoparticles exhibited UV emission peak at approximately 398 nm and three defect peaks corresponding to blue emissions near 435 and 475 nm and to green emission near 490 nm in the PL spectra. The photoluminescence intensity depends firmly on Mn concentrations. The intensity was maximum for low concentrations of Mn and on increasing the Mn concentration further, it decreased together with the broadening of the FWHM as a function of Mn content [12]. The peaks at 465 and 485 nm could be attributed to the transition occurring from Zn interstitials to the valence band, and the peak at 435 nm might be due to the result of the singly ionized oxygen vacancy [13, 14].

ISSN: 2277-9655
Impact Factor: 5.164
CODEN: IJESS7

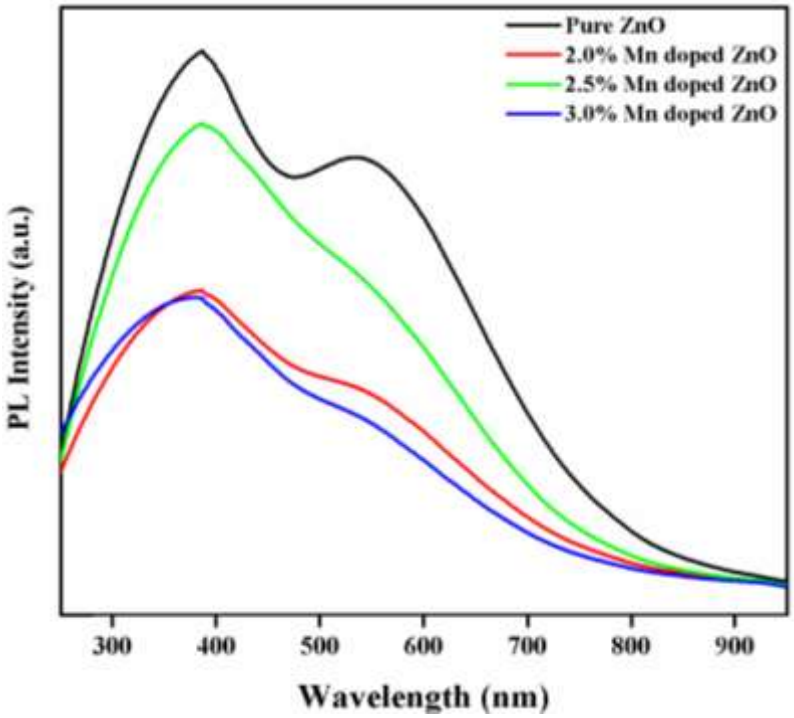


**Figure – 3 Photoluminescence spectra of Pure and Mn doped ZnO nanoparticles**

### 3.4 FESEM Analysis

The morphological information about the pure and Mn doped ZnO nanoparticles were obtained from the FE-SEM. Figure 4 shows the FE-SEM images of the pure and Mn-doped (2.0, 2.5 and 3% Mn) ZnO nanoparticles, respectively. The agglomerated particles neck with their neighbours, and they form hexagonal shapes intermitted with voids, ensuring high surface area [15]. The presence of some bigger particles might be attributed to the aggregation of smaller particles. The particle morphology changes significantly with respect to the incorporation of doping agent [16].

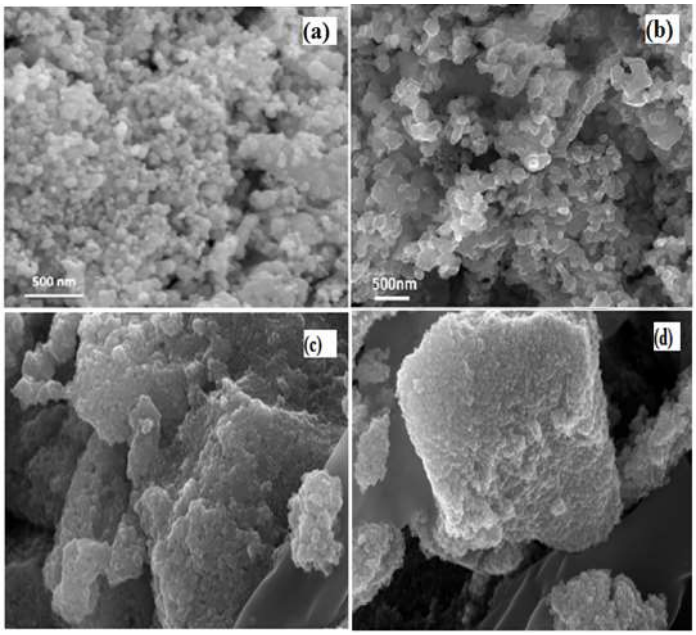


**Figure – 4 FESEM micrographs of Pure and Mn doped ZnO nanoparticles**

ISSN: 2277-9655
Impact Factor: 5.164
CODEN: IJESS7

**3.5 Cell Viability and Cell Penetration by Nanoparticles**

Cell penetration capabilities of five different doses (20, 40, 60, 80 and 100 µg/mL) of each of the four nanoparticles (znsp1, znsp2, znsp3 and znsp4) were tested against the human cervical cancer cells during a total culture period of 4 hours. The obtained results revealed that the 100 µg/mL dosage concentartion of each of the four nanoparticles showed strong cell penetration activity [17] as shown in Figure 5.

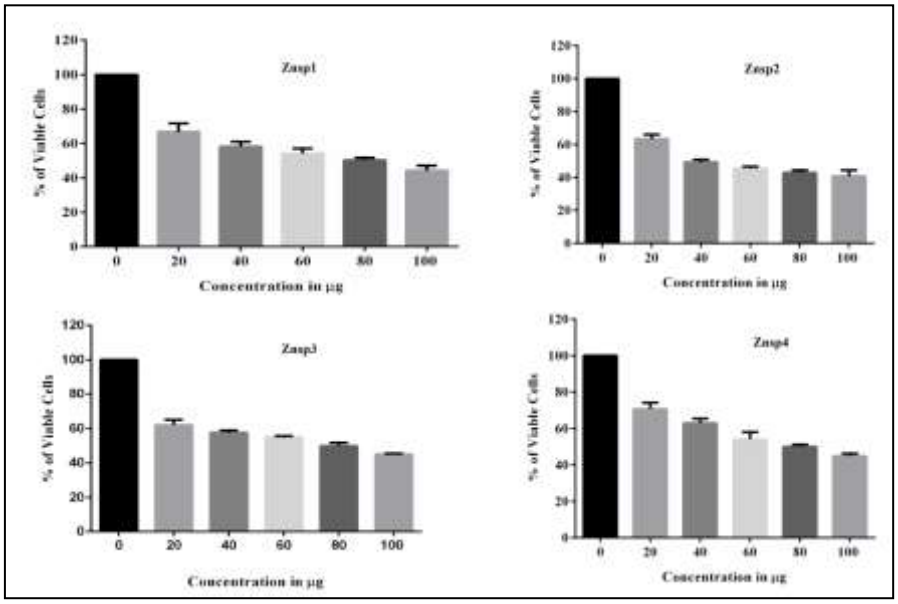


**Figure – 5 Cell penetration & Cell viability percentages of pure and Mn doped nanoparticles on human cervical cancer cells exposed for 24 hours using MTT assay.**

At zero culture time, no trace of any of the four nanoparticles was seen inside the cells. However, after 2 hours, significant amount of nanoparticles penetrated into the cells which can be confirmed by apoptosis represented by the phase contrast micrographic images shown in Figure 6. No further cell penetration activity was observed after the total culture period of 3 hours.

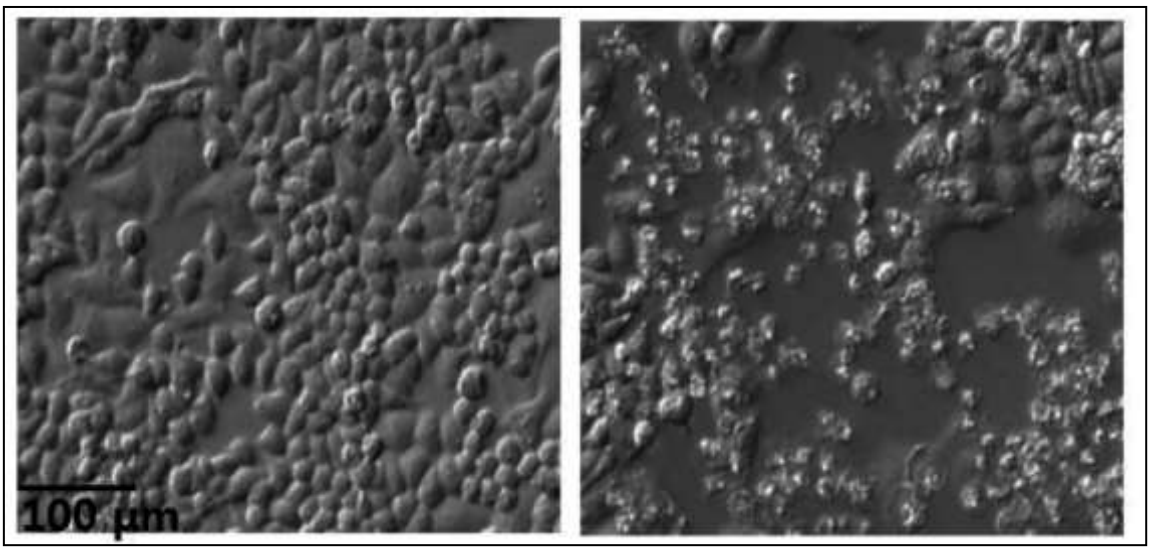


**Figure – 6 TEM images showing the induced cytotoxicity of 2.0% Mn doped ZnO nanoparticles on human cervical cancer cells before and after treatment.**

At lower dosage concentration (20 µg/mL), all the four nanoparticles showed higher cell viability percentage which was shown in Figure 5. On increasing the dosage levels, significant cellular activity (mitochondrial

reductase activity) was observed [18]. Upon increasing the dosage concentration further, the cell viability percentage of all the four nanoparticles decreased. Among the four nanopartiles (undoped and 2.0, 2.5 and 3.0% Mn doped ZnO) 2.0% Mn doped ZnO nanoparticles (coded as znsp2) with a doage level of 100 µg/mL exhibited higher cell killing activity. The effective concentration corresponding to 50% cell viability (EC50) was used to compare the quantitative cytotoxic nature of all the four nanoparticles. Among the four nanoparticles, 2.0% Mn doped ZnO (znsp2) has the least EC50 value 100 µm/mL having 46.25% viable cells [19]. However, 2.5 and 3.0% Mn doped ZnO nanoparticles (znsp3 and znsp4) did not enhance the cell killing activity [20]. From this analysis, it can be proposed that 2.0% Mn doped ZnO plays the dominant role in killing human cervical cancer cells compared to other Mn concentrations.

## IV. CONCLUSION

PEG passivated Pure and Mn doped ZnO nanoparticles were prepared using chemical precipitation method. XRD analysis revelas that the lattice parameters increases with incresing Mn content in ZnO nanoparticles. Reduction in average crystallite size with increasing Mn content was observed and the avergae crystallite size was calculated to be 17.19 nm. This results show that PEG plays an important role in controlling the particles size. UV-Vis DRS spectra exhibited an appreciable shift in the absorption wavelength of Mn doped ZnO nanoparticle compared to the undoped ZnO. Dose dependent cytotoxicity of PEGylated pure and Mn doped ZnO nanoparticles were tested against human cervical cancer cells. Cytotoxicity mechanisms such as Cell viability, nanoparticle cell penetration rate were studied for the as prepared pure and Mn doped ZnO nanoparticles. Compared to undoped ZnO, the Mn doped ZnO nanoparticles showed higher cell killing effect which may be attributed to the combined effect of $Zn^{2+}$ ion release and intracellular ROS generation. It was observed that the best cell killing results were obtained with lowest Mn doping concentrations ie., 2.0% Mn doped ZnO. From our study, it is proposed that 2.0% Mn doped ZnO (znsp2) nanoparticles plays the dominant role in killing human cervical cancer cells compared to other Mn doped ZnO nanoparticles.

## V. REFERENCES

[1] V. Sharma, R. K. Shukla, N. Saxena, D. Parmar, M. Das and A. Dhawan, Toxicology. Letters., 2009 Mar 28;185(3).
[2] D. Das, B.C. Nath, P. Phukon, A. Kalita, S.K. Dolui, Synthesis of ZnO nanoparticles and evaluation of antioxidant and cytotoxic activity, Colloids Surf B Biointerfaces, 111 (2013) 556–560.
[3] S. Ravichandran, D.R. Franklin, U. Kalyan, Effect of capping agent on the synthesis of zinc oxide nanoparticles by precipitation and chemical reaction methods, National J Chem Biosis, 1 (2010).
[4] Y. Yuliah, A. Bahtiar, Synthesis and characterization of PVP-capped ZnO particles and its blend with poly(3-hexylthiophene) for hybrid solar cells application, AIP Conference Proceedings, 1554 (2013).
[5] T. Gutul, E. Rusu, N. Condur, V. Ursaki, E. Goncearenco, P. Vlazan, Preparation of poly(Nvinylpyrrolidone)- stabilized ZnO colloid nanoparticles, Beilstein J. Nanotechnol., 5 (2014) 402–406.
[6] E.R. Arakelova, S.G. Grigoryan, F.G. Arsenyan, N.S. Babayan, R.M. Grigoryan, N.K. Sarkisyan, In vitro and in vivo Anticancer Activity of Nanosize Zinc Oxide Composites of Doxorubicin, International Journal of Medical, Health, Biomedical, Bioengineering and Pharmaceutical Engineering, 8 (2014).
[7] G. Jia, Y. Wang, and J. Yao, Dig J Nanomater Bios 7, 261-67 (2012).
[8] Kim KJ, Park YR. Optical absorption and electronic structure of $Zn_{1-x}Mn_xO$ alloys studied by spectroscopic ellipsometry. J Appl Phys 2003;94:867.
[9] Deka S, Joy PA. Synthesis and magnetic properties of Mn doped ZnO nanowires. Solid State Commun 2007;142:190.
[10] 27. L. L. Yang, Q. X. Zhao, M. Willander, J. H. Yang, and I. Ivanov, J. Appl. Phys. 105, 053503-7 (2009).
[11] K. Vanheusden, C. H. Seager, W. L. Warren, D. R. Tallant, and J. A. Voigt, Appl Phys Lett. 68, 403 (1996).
[12] N. Padmavathy and R. Vijayaraghavan, Sci Technol Adv Mat 9, 035004 (2008).
[13] C. M. Mo, Y. H. Li, Y. S. Liu, Y. Zhang, and L. D. Zhang, J Appl Phys 83, 4389-91 (1998).
[14] J.-S. Lee, K. Park, M.-I. Kang, I.-W. Park, S.-W. Kim, W. K. Cho, H. S. Han, S. Kim, J. Cryst Growth 254, 423- 31 (2003).

ISSN: 2277-9655
Impact Factor: 5.164
CODEN: IJESS7

[15] L. C. Ann, S. Mahmud, S. K. M. Bakhoria, A. Sirelkhatim, D. Mohamad, H. Hasan, A. Seeni, R. Abdul Rahman, Ceram Int. 40, 2993-3001 (2014).
[16] S. Maniv, W. D. Westwood, and E. Colombini, J. Vac. Sci. Technol. 20, 162-70 (1982).
[17] I. Iavicoli , E. J. Calabrese and M. A. Nascarella, Dose-Response, 2010, 8, 501-517.
[18] Z. M. Xiu , Q. B. Zhang, H. L. Puppala, V. L. Colvin and P. J. J. Alvarez, Nano Lett. , 2012, 12, 4271-4275.
[19] M. P. Mattson, Hum. Exp. Toxicol., 2008, 27, 155-162.
[20] C. C. Shen, S. A. James, M. D. de Jonge, T. W. Turney, P. F. A. Wright and B. N. Feltis, Toxicol. Sci., 2013, 136, 120-130.

## CITE AN ARTICLE

Vijayakumar, G., & Bhoopathi, G. (2018). SYNTHESIS, CHARACTERIZATION AND IN VITRO CYTOTOXICITY EVALUATION OF PEGYLATED MN DOPED ZNO NANOPARTICLES ON HUMAN CERVICAL CANCER HELA CELLS. *INTERNATIONAL JOURNAL OF ENGINEERING SCIENCES & RESEARCH TECHNOLOGY*,*7*(5), 139-146.